Research Article

Journal of PeptideScience

Received: 13 November 2009 Revised: 22 March 2010 Accepted: 26 March 2010 Published online in Wiley Interscience: 26 May 2010

(www.interscience.com) DOI 10.1002/psc.1247

Interaction of the prion protein fragment PrP 185–206 with biological membranes: effect on membrane permeability

Sabina Sonkina,[a] Ilnor I. Tukhfatullina,[a] Núria Benseny-Cases,[b] Maksim Ionov,[c] Maria Bryszewska,[c] Bakhtiyar A. Salakhutdinov[a] and Josep Cladera[b]*

Amyloids are proteinaceous aggregates related to the so-called conformational diseases, such as Alzheimer's and prion diseases. The cytotoxicity of amyloids may be related to the interaction of the amiloidogenic peptides or proteins with the cell membrane. In order to gain information on the physico-chemical effects of amyloids on membranes, we have studied the interaction of the human prion amyloidogenic fragment PrP 185–206 with negatively charged model membranes. The results show that the peptide causes the destabilization of the membrane, making it permeable to potassium ions and to charged organic compounds. This effect correlates with the interaction of the peptide with the membrane, causing a variation in the magnitude of the electrostatic surface and dipole membrane potentials. This effect on the electrostatic properties of the membranes may help explaining the observed permeability: a neutralization of the surface negative charge and a decrease of the inside-positive dipole potential would facilitate the translocation of positive ions. The structural analysis of the peptide in the presence of model membranes reveals that it adopts a predominantly unordered structure without any signs of amyloid formation. The results may be relevant in relation to the recently described cell toxic capacity of the peptide. Copyright © 2010 European Peptide Society and John Wiley & Sons, Ltd.

Keywords: amyloid; prion; membrane; PLM

Introduction

The conversion of the prion protein (PrP or PrP^{c}), normally found on the outer surface of neurons, into an abnormal conformer (PrP^{sc}) seems to be a key molecular event in the pathogenesis of Prion diseases. Amyloid aggregates rich in β-sheet structures are found in amyloid plaques in the affected central nervous systems [1,2]. Recent findings on the conversion of PrP^{c} into the pathologic conformation PrP^{Sc} show that the membrane environment can affect the conformational structure and stability of the protein itself [3,4]. It was demonstrated that PrP instantaneously aggregates after interaction with phospholipids, especially with phosphatidylinositol (PI) and phosphatidylethanolamine (PE) [5]. Morillas *et al*. [3] showed that PrP interacting with membranes was particularly strong under acidic conditions. Furthermore, it was also found that amyloidogenic proteins physically intercollate into and penetrate membranes, leading to abnormal permeability [3].

In order to reveal the role of the membrane in protein aggregation and vice versa – the effect of the protein on the integrity of membrane – numerous studies have been carried out using synthetic segments of the prion protein corresponding to different protein regions and their physical and chemical properties and cytotoxicity have been studied.

The PrP 106–126 region has been identified as the most highly amyloidogenic region with neurotoxic activity. It has the capacity to readily form fibrils [6], being partially resistant to proteolysis [7] and a role in neurodegeneration has been proposed based on the modulation of the membrane properties. It was shown that this 21-residue fragment of the prion protein could form ion-permeable channels in planar lipid bilayer membranes [8,9]. However, Henriques *et al*. [10] have found that the fragment PrP 106–126 does not have a strong affinity for lipid membranes under conditions mimicking the cytoplasmic environment. Under conditions that mimic the endosomal environment, the region 106–126 presented a weak tendency to interact with membranes without being able to form pores [10].

Another PrP fragment, comprising the second helical region of the prion protein, PrP 185–206 has been shown to be monomeric at neutral pH and has been described to be able to undergo a nucleation-dependent process ending up in the formation of fibrils, rich in β-sheet structure under physiological conditions as well as at pH 5.5. This fragment was found to be toxic to a 20% of a cell population of a neuroblastoma line [11,12].

* *Correspondence to: Josep Cladera, Unitat de Biofísica i Centre d'Estudis Biofísics, Departament de Bioquímica i de Biologia Molecular, Facultat de Medicina, Universitat Autònoma de Barcelona, 08193 Bellaterra, Barcelona, Spain. E-mail: josep.cladera@uab.cat*

a *Laboratory of Physical and Chemical methods, Institute of Bioorganic Chemistry of Science Academy, Mirzo Ulugbek, 83, Tashkent, Uzbekistan*

b *Unitat de Biofísica i Centre d'Estudis Biofísics, Departament de Bioquímica i de Biologia Molecular, Facultat de Medicina, Universitat Autònoma de Barcelona, 08193 Bellaterra, Barcelona, Spain*

c *Department of General Biophysics, University of Lodz, ul. Banacha 12/16, Lodz 90-237, Poland*

Journal of PeptideScience

In the present paper, we report that the PrP 185–206 prion fragment interacts with negatively charged planar lipid membranes (PLMs). The peptide does not form structurally well-defined ion channels, but rather makes phospholipid bilayers permeable by forming a wide variety of transient and variably sized defects. Fourier-transform infrared spectroscopy (FTIR) experiments using model membranes show that alteration of membrane permeability is caused not by peptide aggregates but rather by monomers or small oligomers. In order to determine the mechanism underlying this permeability changes, differential scanning calorimetry (DSC), infrared spectroscopy, fluorescence spectroscopy and electron microscopy measurements have been carried out using negatively charged phospholipid vesicles. The results show that the alteration of the membrane stability caused by PrP 185–206 may be related to the alteration of the electrostatic properties of the membrane.

Materials and Methods

L-α-Phosphatidylocholine dimyristoyl (DMPC), L-α-phosphatidyl–L-serine (PS) from bovine brain and L-α-phosphatidylocholine (PC) from egg yolk were purchased from Avanti Lipids. Asolectin from soya bean was from Sigma. The fragment 185–208 of the prion protein (DrD185-206) was purchased from JPT, Germany.

Experiments with Planar Lipid Bilayers

The standard buffer used in the planar bilayers (PLMs) experiments contained 0.1-M KCl, 5-mM HEPES at pH 7.4, adjusted with KOH. PLMs were formed from 1.4% solution of asoelctin in *n*-octane across a ~0.2 mm hole in a 25-μm-thick teflon partition separating the two electrolyte solutions, using the method by Muller *et al*. [13]. All experiments were carried out at 25 °C. Membrane formation was monitored visually with a binocular microscope and electronically via the capacity current. The electrical characteristics of PLMs were measured under voltage-clamp conditions as described elsewhere [14]. Ag/AgCl electrodes in 3-M KCl 3% agarose bridges were used both for the application of voltage and recording of the ionic current. The current was measured using an EPC-7 patch-clamp amplifier (HEKA, Germany) and filtered at 3 kHz. The current was converted to voltage, digitized with a sampling frequency of 10 kHz, stored on a computer and analyzed off-line with the analysis of whole-cell and single-channel pClamp data Version 12.1.0.46 (Designed for 32-bit Windows) program (® Gui Droogmans).

Preparation of Large Unilamellar Vesicles

Large unilamellar lipid vesicles (LUVs) for FTIR and fluorescence experiments were prepared according to Mayer *et al*. [15]. PC and PS (20 : 1) (in chloroform/methanol) were mixed in a round bottom flask and dried under a stream of nitrogen gas by rotary evaporation until a thin film of lipids was formed. The film was resuspended in buffer (10 mM Tris pH 7.5 for fluorescence experiments or 10 mM HEPES pD 7.5 for infrared measurements) and then frozen and thawed five times. Finally the vesicle suspension was extruded ten times through two polycarbonate filters of pore size 100 nm using a Liposofast Extruder. Liposomes were always 100 nm in diameter according to control measurements carried out with an Ultrafine Particle Analyzer (data not shown). PC and PS were used in order to carry out the FTIR and fluorescence measurements having the membranes clearly in the fluid phase at 25 °C (the temperature at which the PLMs experiments were carried out.

Labeling of LUVs with FPE and Di-8-ANEPPS

LUVs were labeled exclusively in the outer bilayer leaflet with the surface potential sensor fluorescein-phosphatidylethanolamine (FPE) as described [16]. Briefly, the unilamellar vesicles were incubated with FPE dissolved in ethanol (never more than 0.1% of the total aqueous volume) at 37 °C for 1 h in the dark. Any remaining unincorporated FPE was removed by gel filtration on a PD10 Sephadex G-25 column (Amersham Biosciences) equilibrated with the appropriate buffer. Such a procedure leads to the incorporation of 30–50% of the externally added FPE to the preformed membrane vesicle. The FPE-liposomes were stored at 4 °C until use.

LUVs were labeled with the dipole potential fluorescent sensor Di-8-ANEPPS [1-(3-sulfonatopropyl)-4-(β(2-(di-*n*-octylamino)-6-naphthyl) vinyl) pyridinium betaine] according to a previously described protocol [17,18], by adding the dye at a final concentration of 8 μM (from a stock solution in ethanol) into a cuvette containing LUVs at a final concentration of 300 μM. LUVs were incubated overnight at 37 °C in the dark with the dye to ensure its complete labeling.

Fluorescence Measurements with FPE-labelled Membranes

Fluorescence time courses of FPE-labeled vesicles were measured after adding the desired amount of peptide into 2 ml of lipid suspensions (300 μM lipid) with an SLM-Aminco 8000 spectrofluorimeter. Excitation and emission wavelengths were set at 490 and 520 nm, respectively. Temperature was controlled with a thermostatic bath at 25 °C. The contribution of light scattering to the fluorescence signals was measured in experiments without the dye and was subtracted from the fluorescence traces.

Fluorescence Measurements with Di-8-ANEPPS-labelled Membranes

Di-8-ANEPPS excitation spectra were obtained by exciting the vesicles suspension at 460 nm and collecting their emission at 580 nm [17,18]. Any contribution of light-scattering to the fluorescence signals was corrected from identical recordings with unlabeled membranes. Temperature was controlled with a thermostatic bath at 25 °C.

Vesicle Leakage Measurements

For leakage experiments, release of vesicle contents to the medium induced by addition of the peptide was monitored using the ANTS/DPX assay [19]. Lipid vesicles were prepared in 12.5-mM ANTS, 45-mM DPX, 20-mM NaCl and 10-mM Tris pH 7.5 and were separated from un-encapsulated material by gel filtration in a PD10 Sephadex G-25 column equilibrated with the appropriate buffer and eluted with 10-mM Tris, 100-mM NaCl pH 7.5. Fluorescence measurements were recorded with an SLM-Aminco 8000 spectrofluorimeter. Excitation and emission wavelengths of ANTS were set at 353 and 520 nm, respectively. Temperature was controlled with a thermostatic bath at 25 °C. The 0% fluorescence corresponded to fluorescence of the vesicle at time zero and 100% fluorescence value obtained by adding Triton X-100 (0.5% v/v).

Fourier-transform Infrared Spectroscopy

Infrared spectra of the prion peptide PrP(185–206) (1 mM) as a function of time were acquired in a Mattson Polaris instrument. As much as 400 scans per spectrum were averaged and the buffer

contribution was subtracted. Spectra were acquired every hour for 8 h. Peptide lipid mixtures at a peptide/lipid ratio of 0.05 (M/M) were prepared by mixing the peptide with PC/PS vesicles, prepared as described above. Measurements were carried out at 25 °C.

Differential Scanning Calorimetry

DSC measurements were carried out using a differential scanning calorimeter (DASM-4, Russia) at a heating rate of 1 °C/min. Solutions of pure phospholipids in ethanol were dried in a rotary evaporator. The resulting lipid film on the wall of the flask was hydrated with an appropriate volume of a solution containing the peptide dissolved in Tris 10 mM, pH 7.4 and dispersed by vigorous stirring in a water bath set at 10 °C above the gel–liquid crystal transition temperature of the membrane. The final nominal concentration of lipids in the sample was 0.3 mM for DMPC/PS (95 : 5) mixture systems. All samples were scanned three times, and on the basis of these repetitions it was concluded that the systems were close to equilibrium throughout their phase transitions. There were no indications of any concentration dependence. The total transition enthalpy (ΔH) was calculated from the area under the excess specific heat curve by integration using the Origin Lab Corporation software. The temperature of the phase transition (T_m) was defined as the maximum of the gel-to-liquid crystalline curve. The error was ~0, 05 °C.

Transmission Electron Microscopy

Samples for electron microscopy were prepared by placing 10 µl of of a peptide/lipid solution equivalent to those used for the infrared measurements, for 10 min on a copper grid with a carbon surface and dried with Watman paper. The sample was stained with 2% (w/v) uranyl acetate for 2 min and dried. Transmission electron micrographs were obtained using a Hitachi H-7000 (75 kV) microscope.

Results

PLMs provide a unique environment to assay the activity of membrane active compounds with remarkable sensitivity, through the measurement of the ionic current flowing through a membrane pore. The ionic current recordings shown in Figure 1A suggest that PrP 185–206 affects planar membranes at a concentration of 20 µM causing ill-defined bilayer 'instabilities' rather than distinct, well-defined, channel-like events. Membrane 'instabilities' caused by the peptide had multiple state behaviors with different conductivity. Figure 1 also shows that their gating kinetics were quite fast. Many openings and closings were short and the lifetimes of the events were shorter than seconds. A rather unstructured flickering current was also observed (data not shown).

The current traces presented in Figure 1A also show that 20 µM PrP 185–206 induced ion conductance events at each membrane potentials tested (from −80 to +80 mV) and this conductance events showed a broad range of conductances under symmetrical electrolyte conditions (100 mM KCl). The observed amplitudes of events were comparatively heterogeneous ranging from 10 to 400 pS. Current–voltage curves shown in Figure 1B present an asymmetry which reflects the asymmetry of the peptidic structures in the membranes.

In order to further characterize the destabilizing effects of the peptide we proceeded to study its interaction with negatively charged model membranes using DSC and two fluorescent dyes sensitive to variations of the electrostatic properties of the membrane. The DSC curve of a multilamellar dispersion of DMPC with 5 mol% of PS showed a main transition centered at 22.6 °C. In the presence of the prion fragment PrP 185–206, the transition temperature shifted to 23.8 °C (Figure 2, Table 1). The calorimetric enthalpy slightly decreased and the calorimetric peak became broader by the effect of the interaction with the peptide, as reflected by the value of the width of the band at half height (Table 1). This implies a reduction in the cooperativity of

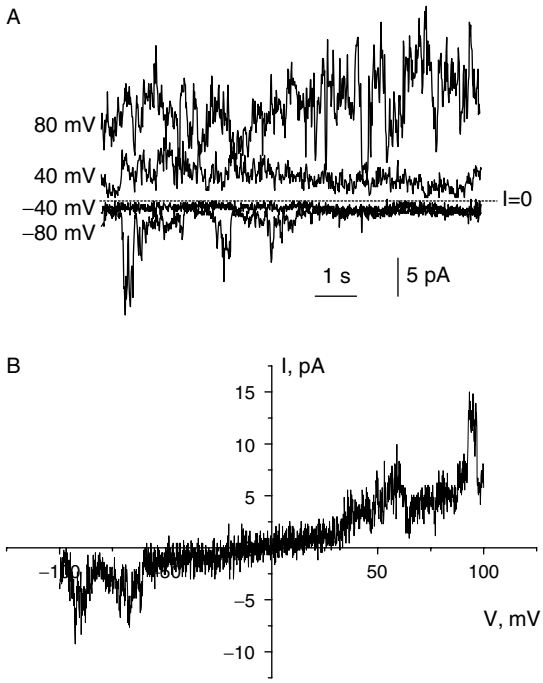

Figure 1. (A) Typical recordings of transmembrane current, induced by PrP 185–206. The peptide (final concentration 20 µM) was added to the *cis*-compartment. (B) Macroscopic conductance induced by PrP 185–206 in planar lipid bilayers. The figure shows the steady-state I–V plot of the membrane containing several channels induced by 20 µM PrP 185–208 at pH 7.4. Temperature was 25 °C.

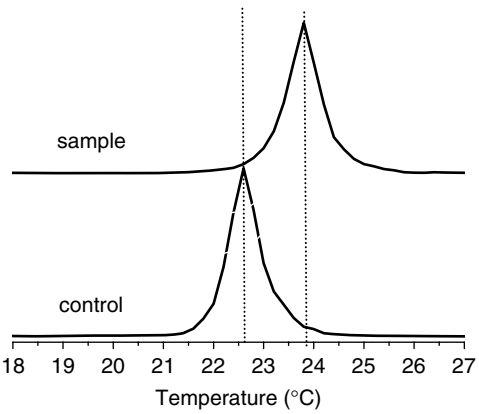

Figure 2. DSC heating thermograms of DMPC/PS (20 : 1) dispersions at pH 7.4 in the absence (control) and presence of PrP 185–206 (upper curve). Peptide/lipid molecular ratio $C_{pep}/C_{lip} = 0.05$. Lipid concentration was 300 µM.

Journal of PeptideScience

Table 1. Calorimetric data relative to (sample 1) DMPC/PS mixture at 95 : 5 ratio; (sample 2) PrP added to DPPC/PS mixture, $C_{pep}/C_{lip} = 0.05$

	Sample 1			Sample 2		
	ΔH_{tot}(kJ mol^{-1})	T_m (°C)	$\Delta T_{1/2}$ (°C)	ΔH_{tot}(kJ mol^{-1})	T_m (°C)	$\Delta T_{1/2}$ (°C)
Scan1	26.73	22.60	0.74	25.50	23.80	0.90
Scan2	–	–	–	25.43	23.80	0.90
Scan3	–	–	–	25.42	23.80	0.90

Experimental values of repeated experiments are given.

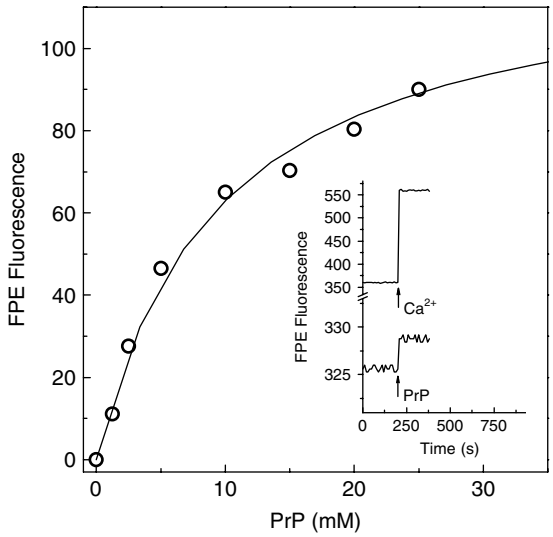

Figure 3. FPE fluorescence as a function of peptide concentration, reflecting the binding of the peptide to the surface membrane; this reduces the membrane surface electronegativity. *Inset*: Fluorescence time-traces illustrating (1) the addition of Ca^{2+} (5 mM), to show that the vesicles have been properly labeled with FPE: addition of positive charges to the membrane surface is expected to increase the FPE fluorescence; (2) the addition of 1 μM PrP 185–206 into an FPE-labeled membrane suspension (PC/PS 20 : 1) causing an increase in the fluorescence of the FPE (the binding curve is the cumulative fluorescence increase caused by successive peptide additions). Lipid concentration was 300 μM. Temperature was 25 °C.

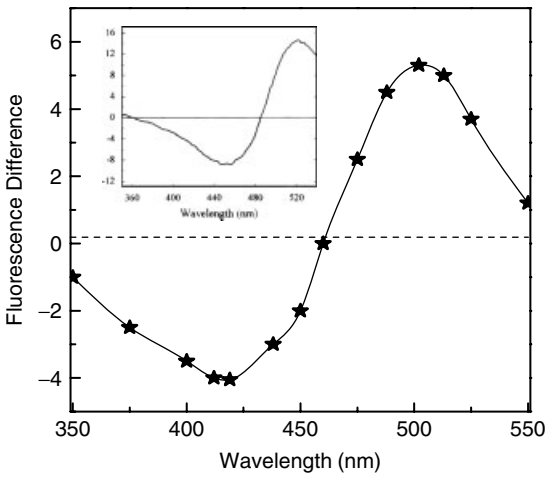

Figure 4. Excitation difference spectrum of vesicles labeled with the dipole potential sensor di-8-ANEPPS. The difference spectrum has been calculated by subtracting the spectrum of a labeled membrane suspension in the absence of the peptide from the spectrum of a labeled suspension (PC/PS 20 : 1 vesicles) in the presence of the peptide. The difference spectrum is compared with the one calculated when the membranes are supplemented with phloretin (inset), a compound known to reduce the resultant membrane dipole moment (positive towards the center of the bilayer). Lipid concentration was 300 μM. Temperature was 25 °C $C_{pep}/C_{lip} = 0.05$.

the thermal transition. The effect of the peptide on the DCS trace is a clear indication of its interaction with the membrane.

This interaction was further characterized by monitoring the binding of the peptide to the membrane surface, using the surface electrostatic potential fluorescent sensor FPE. As shown in Figure 3 (inset) the addition of the peptide (with a net positive charge at neutral pH) to a suspension of PC/PS vesicles labeled with FPE caused an increase of the emitted fluorescence. Such an increase is indicative of a variation in the magnitude of the membrane surface potential due to the binding of the peptide [16]; the membrane surface becomes less negative. The fluorescence variation was used to represent the binding curve shown in Figure 3.

Besides the surface net charges, molecular dipoles present on the lipid molecules contribute to the total electrostatic potential of the membrane. The potential generated by the molecular dipoles has been called the dipole potential and its variations can be monitored using the fluorescent sensor di-8-ANEPPS [17,18]. Figure 4 shows the excitation difference spectrum of PC/PS membranes in the presence/absence of peptide. It can be seen that the spectrum shows a minimum around 420 nm and a maximum around 510 nm. The shape of the difference spectrum is very similar to those generated by the effect of compounds know to change the dipole potential making it less positive towards the center of the lipid bilayer [17] (figure inset). It can be therefore concluded that the interaction of the prion peptide with the model membranes affects the magnitude of the dipole potential by reducing the resultant membrane dipole moment, making it less positive toward the center of the membrane.

We used also the PC/PS model membranes to check whether the peptide would be able to generate the leakage of encapsulated organic compounds. With this purpose we measured the leakage of the encapsulated fluorescent system ANTS/DPX. As shown in Figure 5, the peptide was able to generate a discrete vesicle content leakage (5% of the total amount of encapsulated material), although at a peptide/lipid ratio much higher than the one at which it causes potassium permeability changes. The results, anyway, help corroborating the ability of the peptide to destabilize membranes.

Finally, in order to monitor the structure and the aggregation state of the PrP 185–206 peptide in the presence of phospholipid membranes, we measured its infrared spectrum at the same lipid to peptide ratios at which the DSC measurements were performed. As shown in Figure 6 the infrared spectra of the peptide in aqueous buffer at pH 7.4 present a broad band centered at

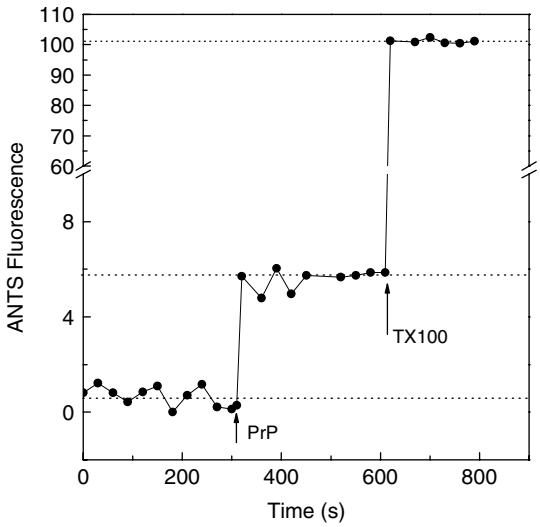

Figure 5. ANTS/DPX release (increase of fluorescence) from the interior of PC/PS vesicles upon addition of PrP 185–206 60 μM. Lipid concentration was 300 μM (PC/PS 20 : 1 vesicles). Peptide/lipid ratio: 0.2. Total solubilization of the vesicles (100% content release) was achieved by adding TX100. Temperature was 25 °C.

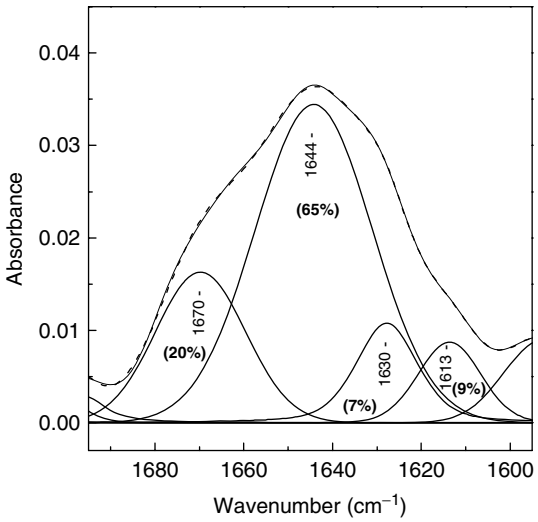

Figure 7. Fitting of component bands to the deconvolved infrared spectra of PrP 185–206 in the presence of PC/PS (20 : 1) membranes. Fourier self-deconvolution was carried out using grams/32 from Galactic Industries. The deconvolution parameters used were, a full width at half height of 15 cm^{-1} and a narrowing factor $k = 1.3$. Fitting of the component bands to the deconvolved spectrum was carried out using the same software.

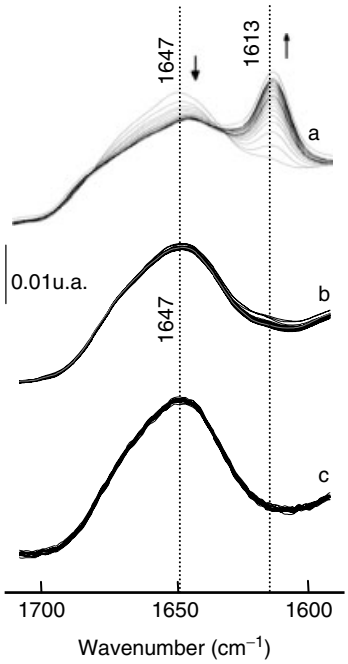

Figure 6. FTIR spectra sequence of PrP 185–206 in the presence of heparin pD 5.5 (aggregating conditions) (A); in the absence of heparin pD 7.5 (B); and in the presence of PC/PS (20 : 1) membranes ($C_{pep}/C_{lip} = 0.05$) pD 7.5. Spectra were acquired every hour during 8 h. Each spectrum is the average of 400 scans.

1644 cm^{-1}, assignable to unordered structures [20]. The spectra are compared to those measured under conditions in which the peptide aggregates (in the presence of heparin, pH 5.5), with the appearance of the characteristic aggregation band at 1613 cm^{-1}. In the absence of heparin at pH 7.5 the spectra did not show any sign of peptide aggregation. In the presence of membranes, the infrared spectra revealed that the peptide remains un-aggregated and no signs of polymerization were observed with time. The infrared spectra in the presence of membranes were deconvolved and curve-fitted in order to resolve the structural secondary components and to make an estimation of the percentages of the different types of secondary structures (Figure 7). Unordered, non-regular structures predominate (65%) with a 20% of turns and just under 10% of beta structures. The fitting corroborates the idea that the peptide is un-aggregated; it has to be considered that an important part of the 9% corresponding to the band at 1613 cm^{-1} may be due to the absorption of lateral chains [21].

Finally, the lack of polymerization of the peptide in the presence of PC/PS membranes was monitored using electron microscopy (Figure 8). No fibrils or any other type of aggregated structures were seen associated to the vesicles.

Discussion

Amyloids are proteinaceous aggregates present in the characteristic plaques detected in the affected tissues of an important number of the so-called conformational diseases. One important aspect of the possible role of amyloids in the toxic events related to the onset and development of the pathologies is their possible action on the cell membrane. Membrane components, such as anionic lipids, ganglyosides or cholesterol, have been shown to be involved at various stages of amyloid aggregation, and in relation to the possible cytotoxic products in pathologies such as Alzheimer's disease and prion diseases [3,22–26].

In the case of the prion fragment PrP 185–206, Mahfoud *et al.* [27] identified it as structurally homologous to the hydrophilic segment 1–28 of the Alzheimer's Aβ 1–40 peptide and a putative binding motif to sphyngolipids. The PLM experiments show that PrP 185–206 induces a wide variety of transient, differently sized defects which serve to compromise the bilayer barrier properties for small electrolytes at relatively low peptide to lipid ratios (around 0.05). At higher ratios the peptide is able to make permeable as well the PC/PS membranes to bigger molecules such as ANTS and DPX. The binding measurements carried out using fluorescent sensors

Journal of PeptideScience

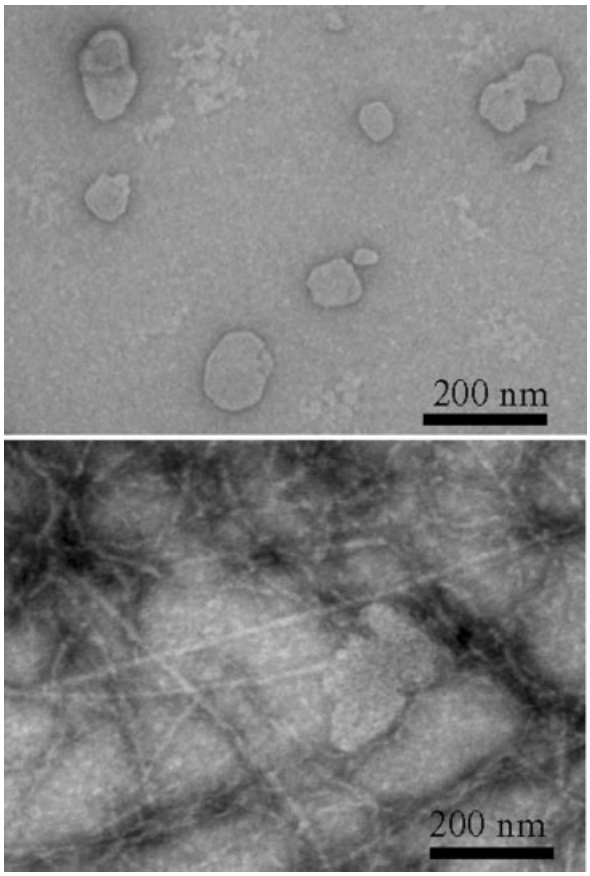

Figure 8. Electron micrographs corresponding to a mixture of PrP 185–206 and PC/PS vesicles (peptide/lipid ratio 0.05) (upper panel) and under aggregating conditions (fibril formation) (lower panel).

of the electrostatic potential to the membrane, indicate that the binding of the peptide to the membrane surface reduces the electronegativity of the surface potential. Moreover, the peptide binding makes the dipole potential less positive toward the center of the bilayer. DSC experiments indicate that the interaction of the peptide with the membrane affects its thermotropic properties. The set of results has brought us to formulate a molecular hypothesis in order to explain the mechanisms by which the peptide could make the membranes more permeable, especially to positive ions. The fact that the peptide neutralizes negative charges on the surface membrane (negatively charged asolectin membranes or PC/PS membranes) and makes the interior of the membrane less positive (reduces the magnitude of the resulting membrane dipole moment, positive toward the center of the bilayer, helps explaining the positively charged ions would have its tendency to remain bound to the membrane surface and it would be easier for them to cross the bilayer (the electrostatic opposition is reduced). In this sense the reduction of the dipole potential could be due to the interaction of the peptide with the PC headgroups. Changes in the orientation of the dipole phosphorous-choline will have direct implications on the resulting dipole moment of the membrane.

One important aspect of this interaction is the aggregation state of the peptide and its structure. PrP 185–206 is known to be able to form amyloid aggregates at pH 5.5 and in the presence of heparin [11,12]. At neutral pH it remains un-aggregated. This is further confirmed by our FTIR measurements (Figure 4A and B). Moreover, the FTIR spectra show that the peptide remains mainly unordered and un-aggregated in the presence of negatively charged model membranes (Figure 4C). The absence of any fibrillar or aggregated species in the presence of membranes is corroborated by the electron micrographs. This means that fibrils and big peptide aggregates can be ruled out as the species responsible for the observed destabilizing effects. The responsible agents have to be either the peptide monomers or small and not quite structured oligomers.

The present work represents another example of the importance of electrostatic interactions between peptide and membranes. In the case of PrP 185–206, the results presented in the present work may be relevant in relation to the recently toxic effect of the peptide in a neuroblastoma cell line [12].

Acknowledgements

This work was funded by the Spanish Ministery of Education and Science (grant BFU2007-64142 to J.C.) and by NATO (Collaborative Linkage Grant CBP.EAP.CLG.981751).

References

1 Prusiner SB, Gabizon R, McKinley MP. On the biology of prions. *Acta. Neuropathol.* 1987; **72**: 299–314.
2 Noinville S, Chich JF, Rezaei H. Misfolding of the prion protein: linking biophysical and biological approaches. *Vet. Res.* 2008; **39**: 48.
3 Morillas M, Swietnicki W, Gambetti P, Surewicz WK. Membrane environment alters the conformational structure of the recombinant human prion protein. *J. Biol. Chem.* 1999; **274**: 36859–36865.
4 Taylor DR, Hooper NM. Role of lipid rafts in the processing of the pathogenic prion and Alzheimer's amyloid-beta proteins. *Semin. Cell Dev. Biol.* 2007; **18**: 638–648.
5 Tsiroulnikov K, Shchutskaya Y, Muronetz V, Chobert JM, Haertle T. Phospholipids influence the aggregation of recombinant ovine prions. From rapid extensive aggregation to amyloidogenic conversion. *Biochim. Biophys. Acta* 2009; **1794**: 506–511.
6 Forloni G, Angeretti N, Chiesa R, Monzani E, Salmona M, Bugiani O, Tagliavini F. Neurotoxicity of a prion protein fragment. *Nature* 1993; **362**: 543–546.
7 Selvaggini C, De Gioia L, Cantu L, Ghibaudi E, Diomede L, Passerini F, Forloni G, Bugiani O, Tagliavini F, Salmona M. Molecular characteristics of a protease-resistant, amyloidogenic and neurotoxic peptide homologous to residues 106–126 of the prion protein. *Biochem. Biophys. Res. Commun.* 1993; **194**: 1380–1386.
8 Lin MC, Mirzabekov T, Kagan BL. Channel formation by a neurotoxic prion protein fragment. *J. Biol. Chem.* 1997; **272**: 44–47.
9 Kagan BL, Azimov R, Azimova R. Amyloid peptide channels. *J. Membr. Biol.* 2004; **202**: 1–10.
10 Henriques ST, Pattenden LK, Aguilar MI, Castanho MA. PrP(106–126) does not interact with membranes under physiological conditions. *Biophys. J.* 2008; **95**: 1877–1889.
11 Klajnert B, Cortijo-Arellano M, Bryszewska M, Cladera J. Influence of heparin and dendrimers on the aggregation of two amyloid peptides related to Alzheimer's and prion diseases. *Biochem. Biophys. Res. Commun.* 2006; **339**: 577–582.
12 Cortijo-Arellano M, Ponce J, Durany N, Cladera J. Amyloidogenic properties of the prion protein fragment PrP(185–208): comparison with Alzheimer's peptide Abeta(1–28), influence of heparin and cell toxicity. *Biochem. Biophys. Res. Commun.* 2008; **368**: 238–242.
13 Mueller P, Rudin DO, Tien HT, Wescott WC. Reconstitution of cell membrane structure in vitro and its transformation into an excitable system. *Nature* 1962; **194**: 979–980.
14 Abramov AY, Zamaraeva MV, Hagelgans AI, Azimov RR, Krasilnikov OV. Influence of plant terpenoids on the permeability of mitochondria and lipid bilayers. *Biochim. Biophys. Acta* 2001; **1512**: 98–110.
15 Mayer LD, Hope MJ, Cullis PR. Vesicles of variable sizes produced by a rapid extrusion procedure. *Biochim. Biophys. Acta* 1986; **858**: 161–168.

16 Buzon V, Padros E, Cladera J. Interaction of fusion peptides from HIV gp41 with membranes: a time-resolved membrane binding, lipid mixing, and structural study. *Biochemistry* 2005; **44**: 13354–13364.
17 Cladera J, O'Shea P. Intramembrane molecular dipoles affect the membrane insertion and folding of a model amphiphilic peptide. *Biophys. J.* 1998; **74**: 2434–2442.
18 Gross E, Bedlack RS Jr, Loew LM. Dual-wavelength ratiometric fluorescence measurement of the membrane dipole potential. *Biophys. J.* 1994; **67**: 208–216.
19 Ellens H, Bentz J, Szoka FC. H+− and Ca2+−induced fusion and destabilization of liposomes. *Biochemistry* 1985; **24**: 3099–3106.
20 Byler DM, Susi H. Examination of the secondary structure of proteins by deconvolved FTIR spectra. *Biopolymers* 1986; **25**: 469–487.
21 Chirgadze YN, Fedorov OV, Trushina NP. Estimation of amino acid residue side-chain absorption in the infrared spectra of protein solutions in heavy water. *Biopolymers* 1975; **14**: 679–694.
22 Bokvist M, Lindstrom F, Watts A, Grobner G. Two types of Alzheimer's beta-amyloid (1–40) peptide membrane interactions: aggregation preventing transmembrane anchoring versus accelerated surface fibril formation. *J. Mol. Biol.* 2004; **335**: 1039–1049.
23 Yip CM, Darabie AA, McLaurin J. Abeta42-peptide assembly on lipid bilayers. *J. Mol. Biol.* 2002; **318**: 97–107.
24 Kakio A, Yano Y, Takai D, Kuroda Y, Matsumoto O, Kozutsumi Y, Matsuzaki K. Interaction between amyloid beta-protein aggregates and membranes. *J. Pept. Sci.* 2004; **10**: 612–621.
25 Wang X, Wang F, Arterburn L, Wollmann R, Ma J. The interaction between cytoplasmic prion protein and the hydrophobic lipid core of membrane correlates with neurotoxicity. *J. Biol. Chem.* 2006; **281**: 13559–13565.
26 Sanghera N, Pinheiro TJ. Binding of prion protein to lipid membranes and implications for prion conversion. *J. Mol. Biol.* 2002; **315**: 1241–1256.
27 Mahfoud R, Garmy N, Maresca M, Yahi N, Puigserver A, Fantini J. Identification of a common sphingolipid-binding domain in Alzheimer, prion, and HIV-1 proteins. *J. Biol. Chem.* 2002; **277**: 11292–11296.

